

# Obsidian hydration dating by SIMS-SS: Surface suitability criteria from atomic force microscopy

I. Liritzis,<sup>a\*</sup> M. Bonini<sup>b</sup> and N. Laskaris<sup>a</sup>

Obsidian artefacts used by prehistoric people could be dated by the SIMS-SS method. However, the method contains some limitations regarding the degree of smoothness of the surface. The presence of wells, cracks, pits, crystals and/or crests induce errors in the dating. Here, we briefly introduce the SIMS-SS method and provide first images of the atomic force microscopy (AFM) of obsidian surfaces and discuss the impact of AFM results on the SIMS-SS dating. The presented dating is straightforward for flat regular surfaces and problematic for irregular surfaces. Copyright © 2008 John Wiley & Sons, Ltd.

**Keywords:** SIMS; obsidian; dating; AFM; hydration; roughness

## Introduction

### SIMS measurements and sample preparation

Secondary ion mass spectrometry (SIMS) analyses were conducted at the commercial laboratory of Evans East, East Windsor, NJ, USA, and the profiles were collected using PHI Model 6300 and 6600 quadrupole-based secondary ion mass spectrometers. A 5.0 KeV Cs<sup>+</sup> primary ion beam with an impact angle of 60° with respect to surface normal was used and negative secondary ions were detected. Charge build-up during profiling was compensated for by use of an electron beam. The ion signal was maximised by using the electron beam resulting in the least amount of charging. The measurements were performed using a 300 × 300 micron ion beam raster, which results in very little visual disruption to the sample surface. Generally, the SIMS depth-scale accuracy for archaeological samples is within 5–10%. This translates into an estimated error of ±0.05 μm. This value is not equivalent to the ±0.01–0.03 μm standard deviation usually associated with SIMS because of the irregular surface topography present on naturally cleaved samples.

There is no treatment of the samples prior to analysis. Small samples are pasted to a sample holder using silver paste. In order to dry the paste the samples and holders are baked in an oven at about 60 °C for 1 h. This also removes any surface water film or organic film. The base pressure of Evans East system is about 7E-10 torr. When the ion source is running, the chamber pressure is typically about 2E-9 torr. The sputtering rate used to measure our samples was 24 Å/s, which is fairly typical. Conversion of ion counts to concentrations is done using an ion implanted obsidian standard. The same material is used to calibrate the sputtering rate, and therefore, there are no direct crater depth measurements of archaeological samples. This method provides very good control of the depth scale and avoids the problems of direct measurement of a rough surface. For polished test samples crater depths are measured using a Dektak 6M stylus profilometer which is reproducible to within 1% on flat, well-controlled samples<sup>[1]</sup> (Dr Steve Novak, pers. comm.)

### SIMS profile and modelling of water diffusion

There are problems in accurately tracking diffused water. SIMS is among the variety of high-precision, non-optical, depth-profiling techniques for measuring the width of the hydration rim. The measurement of the hydration rim with an optical microscope has been proved inaccurate due to microlite inclusions and birefringence.<sup>[2]</sup>

Moreover, the hydration front measured more accurately by SIMS, expected at least partially from Fick's law of diffusion,<sup>[3]</sup> may induce problems with respect to modelling of the sigmoid profile of the entire diffused water. These include; sputtering from ion beam, presence of inclusions, surface topographic anomalies, fissures and cracks, and the mechanism for transport of water in the essentially two regions of sigmoid – the surface near flat 1 region, gradually reduced, and the Fickian diffusion with an exponential variation ending to the tail<sup>[3]</sup> region 2 (see, regions 1 and 2 in Figs 3 and 6).

It is known that depth resolution is limited by atomic mixing effects and the flatness of the analysed area and the dynamic range of depth profiles is limited by crater-edge effects, neutral-beam effects and several types of instrumental background.<sup>[4]</sup> Irregular and/or inhomogeneous surfaces cause problematic diffused regions and, therefore, produce uncertain ages. Water molecules find various paths to diffuse in a non-homogeneous manner, as the size-dependent mechanism relevant to our model<sup>[5]</sup> assumes that water molecules of radius  $r_w = 0.15 \mu\text{m}$  occupy interstitial sites of the obsidian and pass through 'doorways' of radius  $r_D$  jumping from the 'doorway' to another.<sup>[5]</sup> The  $r_D = 0.10 \mu\text{m}$  derives from

\* Correspondence to: I. Liritzis, Laboratory of Archaeometry, Department of Mediterranean studies, University of the Aegean, 1 Demokratias Ave., Rhodes 85100, Greece. E-mail: liritzis@rhodes.aegean.gr

a Laboratory of Archaeometry, University of the Aegean, 1 Demokratias Ave., Rhodes 85100, Greece

b CSGI, Department of Chemistry, Room # 18, via della Lastruccia, 3, 50019 Sesto Fiorentino (FI), Italy

equation regarding activation energy  $E$  which is recognised as the elastic energy to dilate a spherical cavity from radius  $r_D$  to  $r$ . Thus, cavities, holes and troughs of surface topological anomalies will have an impact by distorting initial SIMS profiles which includes the surface saturation (SS) layer. Moreover, these surface anomalies also reflect on the diffusion coefficient ( $D$ ), which in turn depends on the composition of the obsidian, and on the physical nature of the material e.g. pores etc. The obsidian structure reflected in density depends on the bulk composition and connate water, and water diffusivity depends on these factors. However, in the emerged pattern for safe location of SS, there are cases where the location of SS and/or the polynomial fitting of the profile are both problematic. The uncertain ages are linked to the surface topography. An approach to such problems is the use of atomic force microscopy (AFM). This is a well-suited technique in the roughness analysis of obsidian surfaces<sup>[6,7]</sup> and the maximum investigated area of  $100 \times 100 \mu\text{m}$  is representative of the sample. As SIMS profiles are taken with a  $200 \times 200 \mu\text{m}$  ion beam raster large enough to include narrower topological anomalies, the acquisition of SIMS H<sup>+</sup> profiles containing all the above mentioned causes for a distorted profile, resulted occasionally to problematic ages.

### SIMS-SS dating method

The dating of obsidian artefacts is made: (i) by the conventional obsidian hydration dating based on empirical equation  $x^2 = k \times t$  ( $x$  = hydration depth,  $t$  = time,  $k$  = diffusion rate), and (ii) by modelling the sigmoid H<sup>+</sup> profile of the diffused water, in hydrated obsidian surfaces, produced by SIMS, and making use of the SS layer (SIMS-SS).<sup>[5]</sup> In fact, the water diffusion mechanism in obsidian has been revisited with the advent of the latter new dating approach employing SIMS. The H<sub>2</sub>O concentration *versus* depth profiles are modelled, following Fick's law of diffusion, which together with the concept of the SS layer, and the empirical effective diffusion coefficient produces a *phenomenological dating approach* in obsidians<sup>[5]</sup> that provides a sound basis for the new diffusion age equation (SIMS-SS) supported by dated world examples.<sup>[1,5,8]</sup> This age equation depends on the H<sup>+</sup> concentration ( $C_s$ ) and the hydration depth ( $X_s$ ) at SS, the connate or internal water ( $C_i$ ), the diffusion coefficient ( $D$ ), and polynomial coefficients derived from the 3rd degree polynomial fitting of sigmoid curve.<sup>[1,5,8]</sup> SIMS-based dates for more than 40 obsidian specimens from the world over, dating back to well-known ages ranging from 600 to 30 000 years ago, have been compared with radiocarbon dated ages. The convergence between the two dating methods is excellent; a fact that reinforces the new dating approach. However, the determination of the SS layer, i.e. the little flat (plateau) segment in the diffused region of the sigmoid curve, is a crucial age parameter. This SS layer forms with a highest concentration as a progressive front during the diffusion time defined by  $C_s$  and  $X_s$ . This is located by, (i) the sliding progressive regressions to determine a near-zero slope, and (ii) through repeated derivatives approach starting from the initial points to the whole diffused region. This way an emerged pattern for safe location of SS appears. However, the latter has shown cases where the location of SS and/or the polynomial fitting of the profile are both problematic, and uncertain ages are linked to the surface topography.

Here we present a detailed surface investigation with AFM of 2D and 3D images of a selected few from among a dozen prehistoric obsidian tools from the Aegean area (Islands of Yiali, Youra, Mykonos, the Sarakinos cave at central Greece) and Asia Minor (NW Turkey).

## Obsidian Surface Analysis by AFM

### AFM experiments

AFM imaging was performed with an Explorer TMX 2000 microscope (Topometrix) using a  $100 \times 100 \mu\text{m}$  xy,  $10 \mu\text{m}$  z air scanner, and a silicon 'V'-shaped cantilever with an integrated pyramidal tip for contact imaging. Images were taken at room temperature in contact mode, and they were processed by flattening in order to remove the background slope. The scanner used to perform the measurements has a maximum z excursion of  $10 \mu\text{m}$ , corresponding to the maximum difference in the height scale of the sample that could be accessed with our instrument: i.e. the samples presenting gaps bigger than  $10 \mu\text{m}$  cannot be imaged by our instrument. In all the investigated obsidians, the surface profile was fairly irregular, with deep voids and cracks randomly distributed over smoother areas. Holes do not show a regular shape, and also the depths are not homogeneous, ranging from a few tens of nanometers up to a maximum of about  $1 \mu\text{m}$ . The almost-flat areas consist of globular structures with a typical diameter of the smaller sub-units ranging from 50 to 100 nm.

Details in the nano- and microscale observed on the surface could not be detected using Polarised Light Microscope or Scanning Electron Microscope. These features consisted of cracks and voids, which were sometimes within the first  $10 \mu\text{m}$  of the tool surface. In our thesis, this would make any SIMS measurement problematic if the opening was inadvertently targeted, because the missing of initial points from normal diffusion makes modelling of the H<sup>+</sup> *versus* depth profile inadequate for accurate age estimation. However, there are some areas free of crystals, voids and cracks, and these regions are ideal for SIMS.

In view of the SIMS analysis, such samples appear to be reliable with the condition that the spot investigated by the SIMS is in the flat region. Since the size of the holes is always larger than  $1 \mu\text{m}$ , this could be ensured by using an optical microscope to choose the right position on the sample.

## Results and Discussion

Figure 1(a) shows representative images for MYC-1. In particular, an accurate analysis of a *ca* 7.2 micron path along the X-axis well illustrates this morphology: four main subsidence (holes) with the following depths are present from left to right: *ca* 550, 800, 600 nm and close to this last *ca* 350 nm. The holes in this sample, in general, have no regular shape and their depths are not homogeneous, ranging from a few tens of nanometers up to a maximum of about  $1 \mu\text{m}$  (Fig. 1(b)). These morphologies are also present in other regions of the sample (Fig. 1(b, c)). In particular, Fig. 1(c) shows at least two or three troughs and hills of similar depth/height. The almost-flat areas are constituted by globular structures with a typical diameter of the smaller sub-units ranging from 50 to 100 nm. Figure 1(d) gives a 3D representation in graded colour scale using novel software for AFM image processing in matlab. This program converts the RGB coloured AFM image into greyscale and initially represent this image in 3 dimensions by using the number of pixels as x and y axis and the grey-scaling as z axis, and then converts the number of pixels to micrometers of x and y, and the scaling of gray to nanometers of height (z axis).

In order to evaluate the reliability of SIMS measurements, some parameters quantitatively accounting for the morphology of the investigated obsidians are needed. In this context, the surface roughness represents a crucial factor in view of correlating

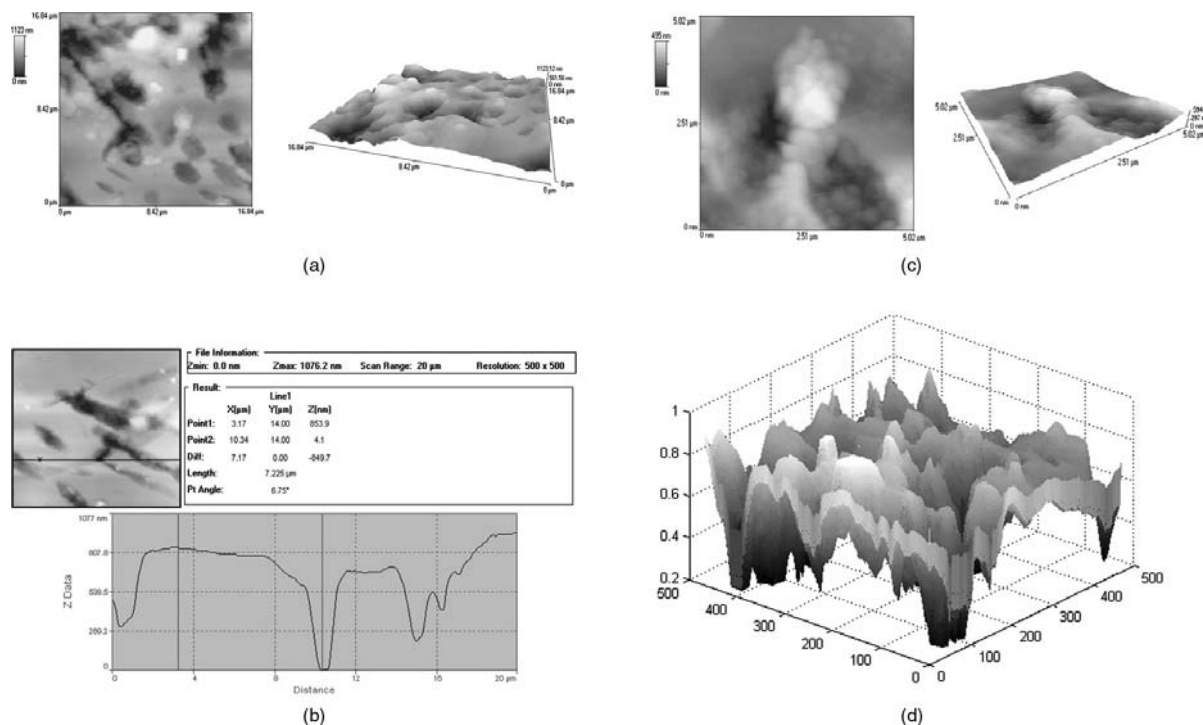


**Figure 1.** (a) Topography image (left) and its three-dimensional representation (right) of a  $16.84 \times 16.84 \mu\text{m}$  spot of the MYC sample, (b) Line profile analysis of a  $20.00 \times 20.00 \mu\text{m}$  spot of the MYC sample, (c) Topography image (left) and its three-dimensional representation (right) of a  $5.02 \times 5.02 \mu\text{m}$  spot of the MYC sample (d) 3D representation of Fig. 1(a) (left). The x and y axis are pixels and z is colour scale.

the accuracy of the dating method with the morphological characteristics of the samples. Although AFM is a well-suited technique in the roughness analysis of surfaces, however, it is well known that roughness as obtained by AFM is influenced by experimental parameters, such as tip radius, tip-sample force, the scan size and pixel resolution. Therefore, in order to make a comparison between different samples, the same scan size, pixel resolution, tip geometry and radius, and tip-sample force were used for all the images that were used to calculate roughness values.

The list of the samples investigated by AFM is reported in Table 1. The roughness parameters which indicate the typical size of the irregular surface features, and surface area/projected area ratio (indicating amount of irregular features in the defined area) of each sample are shown. Arithmetical mean deviation ( $R_a$ ) and root mean square deviation ( $R_{ms}$ ) typically ranges from a few nm to less than 100 nm, while the surface-to-projected area ratios between 1.011 and 1.142, and irregularity,<sup>[9,10]</sup>  $I_{rr}$  (calculated as an alternative to  $R_a$  using the novel program mentioned before.  $I_{rr}$  was calculated by converting the grey-scaling of the  $m \times n$  pixels image to nanometers and calculating the standard deviation of the  $m \times n$  matrix) follows  $R_a$  and  $R_{ms}$ . For the sake of clarity, the same results are shown in Fig. 2 as histograms. The roughness is corroborated by these parameters ( $R_a$ ,  $R_{ms}$ ,  $I_{rr}$ , Area ratios).

According to the obtained results, there is a group of samples where the dating process should be fairly safe, as the surface is reasonably smooth. Namely, the samples that can be included in this group are: YAL-1, DL-90, TURK-6, and YR-3. In the case of the other samples, the spot where the SIMS experiments are performed should be chosen carefully. In particular, the FIKIRTEPE-7 samples look like the most unreliable among the

**Table 1.** Roughness parameters from prehistoric obsidian tool surfaces derived from AFM. MYC for Mykonos, Ulucak near Smyrna, YAL for Yiali, Turk & Fikirtepe for Asia Minor, SAR for Sarakinos cave, YR for Youra Cyclop's cave

Sample	$R_a$ [nm]	$R_{ms}$ [nm]	Surface Area/ $\mu\text{m}^2$	$I_{rr}$ [nm]
MYC-1 (DL-2000-155)	27.66	34.1	1.114	64
ULUCAK (RHO-20-3)	36.56	53.05	1.025	38
YAL-1	13.47	17.14	1.021	17.6
DL-90-282	4.08	5.89	1.008	2.69
TURK-6	7.11	10.37	1.012	9.56
SAR-2	27.63	36.27	1.036	35.36
FIKIRTEPE-7	62.89	82.2	1.142	61.97
YR-3	6.78	9.27	1.012	5.72
MYC-7	25.67	31.6	1.011	18

set of investigated obsidians. It is interesting to note that the sample YR-3, which was macroscopically the less homogeneous, is among the group of the most regular ones, when the macroscopic irregularities are avoided. We can, therefore, conclude that the proper choice of the spot where SIMS analysis is performed represents a crucial step in the reliability of the proposed dating method. When this condition is properly fulfilled, the accuracy of the results should directly depend on the roughness of the sample.

An indication of the correlation between SIMS-diffused profile properties and surface roughness aids selection of appropriate obsidian surfaces for dating. Figure 3 is a sigmoid profile of obsidian by SIMS indicating the diffused region. In the diffused region a linear regression fit ( $y = a + bx$ ) defines the dispersion,

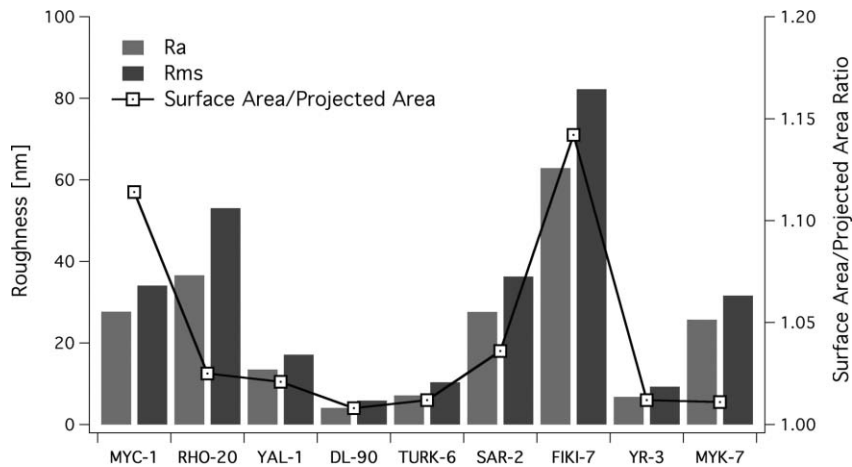


**Figure 2.** Roughness (Ra, Rms) in nm and Area ratios factor for all examined samples.

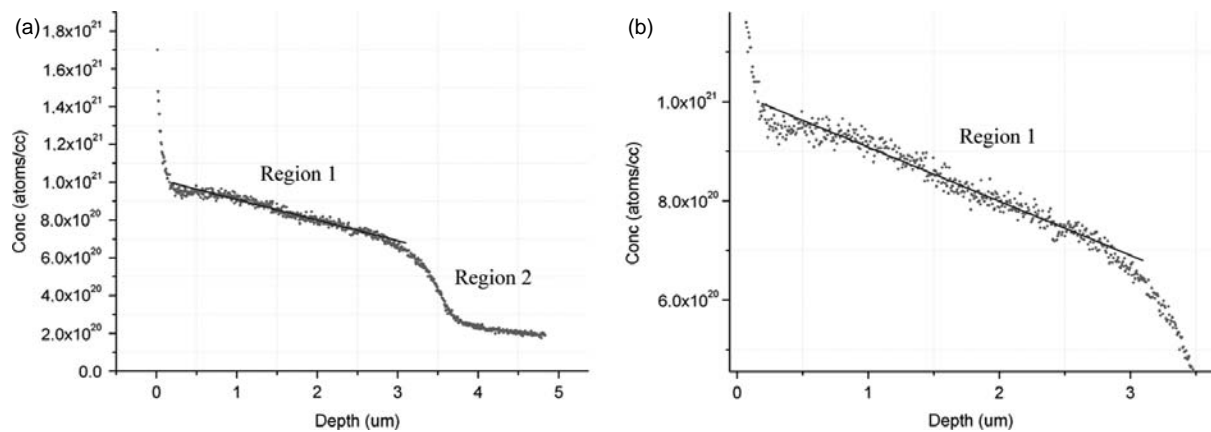


**Figure 3.** (a) SIMS profile of YR-2 from Yali island, with the linear regression in the diffused region and (b) a more detailed image of the diffused region, Diffusion regions 1 and 2, are shown (see text).

which reflects the degree of roughness and sputtering (Fig. 3(b)). The dispersion is defined by the Standard Deviation of Residuals (Rstd) (Fig. 4).

These are correlated with AFM factors, based on the rationale that the smoother the surface the less the dispersion and smoother the SIMS diffusion profile.

In Fig. 5 the factor Rstd is plotted in relation to  $I_{rr}$  και Ra. It is interesting to note a linear relationship between these factors, which represent SIMS and AFM results, implying a clear interdependence.

The effects of surface anomalies and/or removed flakes on the SIMS-SS dating is apparent in the following age calculations.

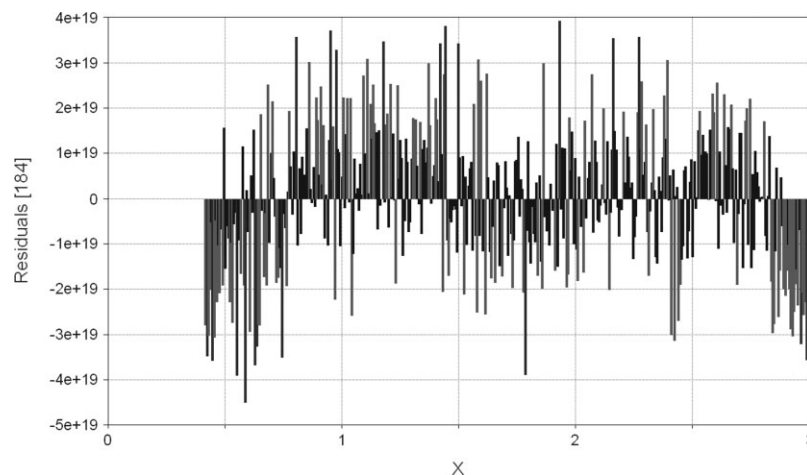


**Figure 4.** Residuals of linear regression fit in the diffused region of Fig. 3.

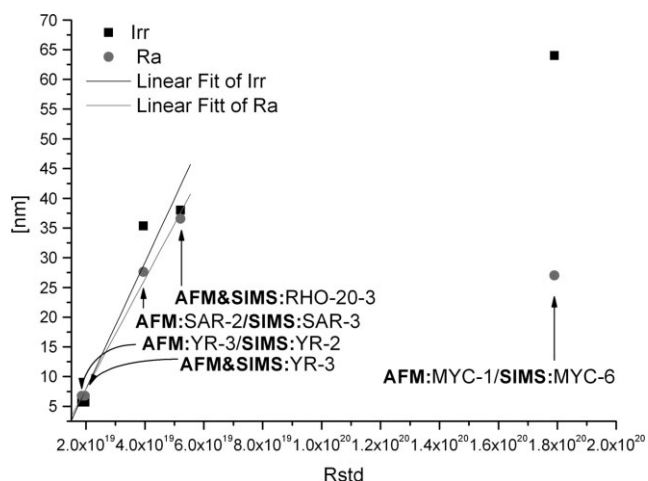


**Figure 5.** Irr and Ra plotted against Rstd.

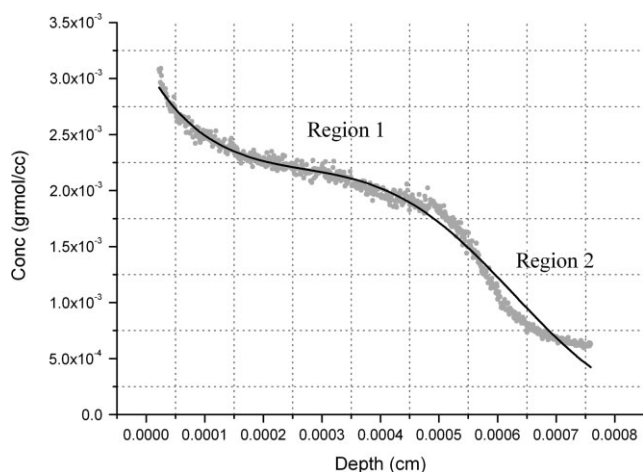


**Figure 6.** SIMS profile of YAL-2 sample (points) and the 3rd order fitting polynomial (line) with  $Rsq = 0.98$ . Diffusion regions 1 & 2 are indicated (see text).

### AFM Impact on SIMS-SS Dating

Table 2 shows SIMS-SS parameters of age equation for five obsidian blades of different origin: Aegean Islands, Asia Minor and Mainland Greece. All ages span the Greek Mesolithic to Neolithic period (about 12 000–4000 years B.C.). Figure 6 shows the profile and fit for YAL-2. The SAR-3 has great dispersion in the diffused region, presumes loss of some initial surface (Fig. 7). Another sample from MYC-1 (Mykonos Island, Ftelia Neolithic settlement) shows a surface not smooth and with many rugosity features (Fig. 1(a–d)). Also, the correlation with the Rstd factor from SIMS (SIMS sample MYC-6) as shown in Fig. 5 is out of linearity. This implies that the sample is not datable. The SAR-3 has great dispersion in the diffused region, presumes loss of some initial surface (Fig. 7), and is not datable. SAR-4, despite the two little tops at around 1 and 1.8 micron (Fig. 8) the successive regression and derivatives procedures define the SS and age.

### Conclusion

SIMS-SS age determinations have the potential for producing ages within the last millennia, and thus, useful for prehistoric

**Table 2.** SIMS-SS parameters of age equation for five obsidian blades

Sample	$C_s$ (gmol/cc)	$X_s$ ( $\mu$ m)	$C_{int}$ (gmol/cc)	$D$ ( $cm^2$ /year)	$e^k$	Age (SIMS) Years before present (BP)	Age (archaeol.) Years before present (BP)
YAL-2 Yali Island, Greece	$0.002498 \pm 2.4358E-005$	$0.000103347 \pm 2.11704E-006$	$0.00062309 \pm 1.50414E-005$	$3.5246E-12$	240	$6022 \pm 245$	$7000-5000$ .
YR-2 Youra Island, Cyclops cave	$0.0007930 \pm 1.30E-5$	$2.612E-5 \pm 2.19E-6$	$0.000158 \pm 5.52E-6$	$1.92E-12$	540	$12636 \pm 780$	$14000-10000$
YR-3 Youra Island, Cyclops cave	$0.0005165 \pm 8.69E-6$	$0.00011835 \pm 4.04E-6$	$5.5296E-5 \pm 3.18E-6$	$2.3621E-13$	40	$13212 \pm 2054$	$14000-10000$
ULUCAK Neolithic Settlement near Smyrna, Asia Minor	$0.001814 \pm 3.36E-5$	$0.0001764 \pm 3.19E-6$	$0.0002148E-5 \pm 1.16E-5$	$5.15E-13$	10	$6686 \pm 298$	$\sim 7000$
SAR-4 Sarakinos cave	$0.0009746 \pm 1.53E-5$	$0.0001283 \pm 3.6E-6$	$0.000149 \pm 7.30E-6$	$4.73E-13$	60	$14075 \pm 1764$	$12000-10000$

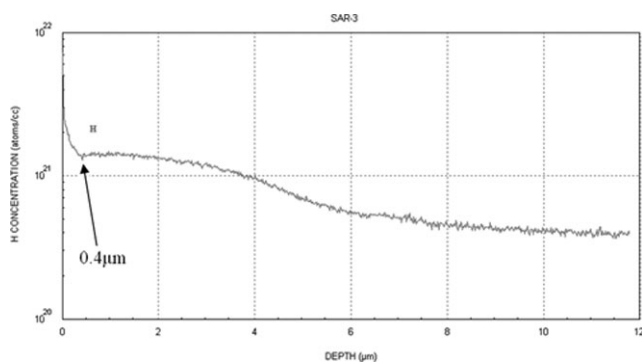


**Figure 7.** SAR-3 SIMS profile. The non-sigmoid start of the profile at 0.4  $\mu\text{m}$  depth and the great dispersion in the diffused region strongly indicate the loss of initial surface flake.

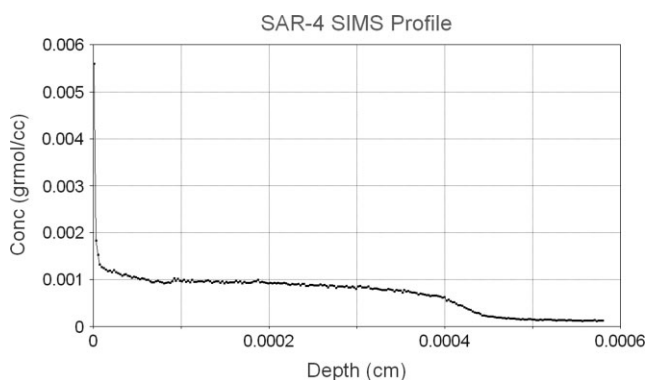


**Figure 8.** SAR-4 SIMS profile. Two little tops are detectable at 1 and 1.8 micron but the sample remains datable.

investigations. However, the SIMS H<sup>+</sup> profiling is very susceptible to the surface conditions, most of which reflect the inner status

of the obsidians. From the present work one can state that SIMS measurements on the variety of examined samples will provide meaningful results, as long as the spot selected for the SIMS profile acquisition is chosen with the aid of an optical microscope in a way to avoid the micron-scaled inhomogeneity of the sample. However, in a few cases, these surface conditions are not easily spotted or may be erroneous. An indication of the linear correlation between SIMS-diffused profile properties and surface roughness measured by AFM reconfirms the interdependence. This aids selection of appropriate obsidian samples/surfaces for dating.

It is interesting to note that samples which were macroscopically less homogeneous, are among the group of the most regular ones, when the macroscopic irregularities are avoided. We can, therefore, conclude that AFM images are very important data for proper choice of the spot where SIMS analysis is performed, which in certain cases was not so easy to find. They represent a crucial step in the reliability of the obtained ages. When this condition is properly fulfilled, the accuracy the results and suitability of the samples should directly depend on the roughness of the sample.

## References

- [1] Liritzis I, Diakostamatiou M, Stevenson CM, Novak SW, Abdelrehim I. *J. Radioanal. Nucl. Chem.* 2004; **261**(1): 51.
- [2] Stevenson CM, Liritzis I, Diakostamatiou M. *Mediterr. Archaeol. Archaeom.* 2002; **2**(1): 93.
- [3] Brodkey R, Liritzis I. *Mediterr. Archaeol. Archaeom.* 2004; **4**(2): 67.
- [4] Magee CW, Honig RE. *Surf. Interface Anal.* 1982; **4**(2): 35.
- [5] Liritzis I. *Archaeometry* 2006; **48**(3): 533.
- [6] Simpson JG, Sedin LD, Rowlen LK. *Langmuir* 1999; **15**: 1429.
- [7] Kiely JD, Bonnell AD. *J. Vac. Sci. Technol., B* 1997; **15**: 1483, Topometrix SPMLab Software, version 3.05.
- [8] Liritzis I, Ganetsos T. *Appl. Surf. Sci.* 2006; **252**(19): 7144.
- [9] Poon CY, Bhushan B. *Wear* 1995; **190**: 76.
- [10] Chen Y, Huang W. *Meas. Sci. Technol.* 2004; **15**: 2005.